



Multi-Omic Assessment of Blood and Tissue of Renal Cell Carcinoma Patients Provides a Comprehensive Characterization of the Systemic and Local Immune Response

Qanber Raza, Nick Zabinyakov, Ling Wang, Lauren Tracey, Thomas D. Pfister, Liang Lim, David King, Christina Loh
Standard BioTools Canada Inc., Markham, ON, Canada

Introduction

Clear cell renal cell carcinoma (ccRCC) represents a biologically heterogeneous malignancy with diverse tumor and immune microenvironment interactions that influence disease progression and therapeutic response. Traditional profiling using a single technology obscures the real disease biology critical for understanding tumor-immune dynamics. Recent advances in spatial multi-omic technologies enable simultaneous mapping of transcriptomic and proteomic features within tissues and blood derived from individual patients. This study aims to comprehensively characterize the immune and oncological landscape of ccRCC using integrated multi-omic approaches to identify systemic response, microenvironmental niches, immune cell states and tumor heterogeneity that underpin immune evasion and therapeutic resistance. Specifically, our findings support the development of spatially informed biomarkers and targeted therapies to improve precision medicine approaches for ccRCC treatment.

Methods and materials

We took an integrative approach of mapping localized and systemic immune cell responses in ccRCC patient samples from Stage 1 and Stage 3 patients (Figure 1). We employed CyTOF™ technology to profile peripheral blood mononuclear cells (PBMC) and tumor-derived cells (TDC) using a 50-plus-antibody panel. We obtained matched FFPE tumor tissue sections and performed spatial transcriptomics using the Xenium 5K assay (Xe5K; 10X Genomics) and hematoxylin and eosin (H&E) staining followed by spatial proteomics using Imaging Mass Cytometry™ (IMC™) technology with a 43-marker immunology-focused antibody panel on the same tissue section. We combined the datasets for all modalities to explore tumor and immune-related signatures associated with specific stages of disease as well as correlation of immune cell phenotypes in systemic circulation compared with tumor tissue.

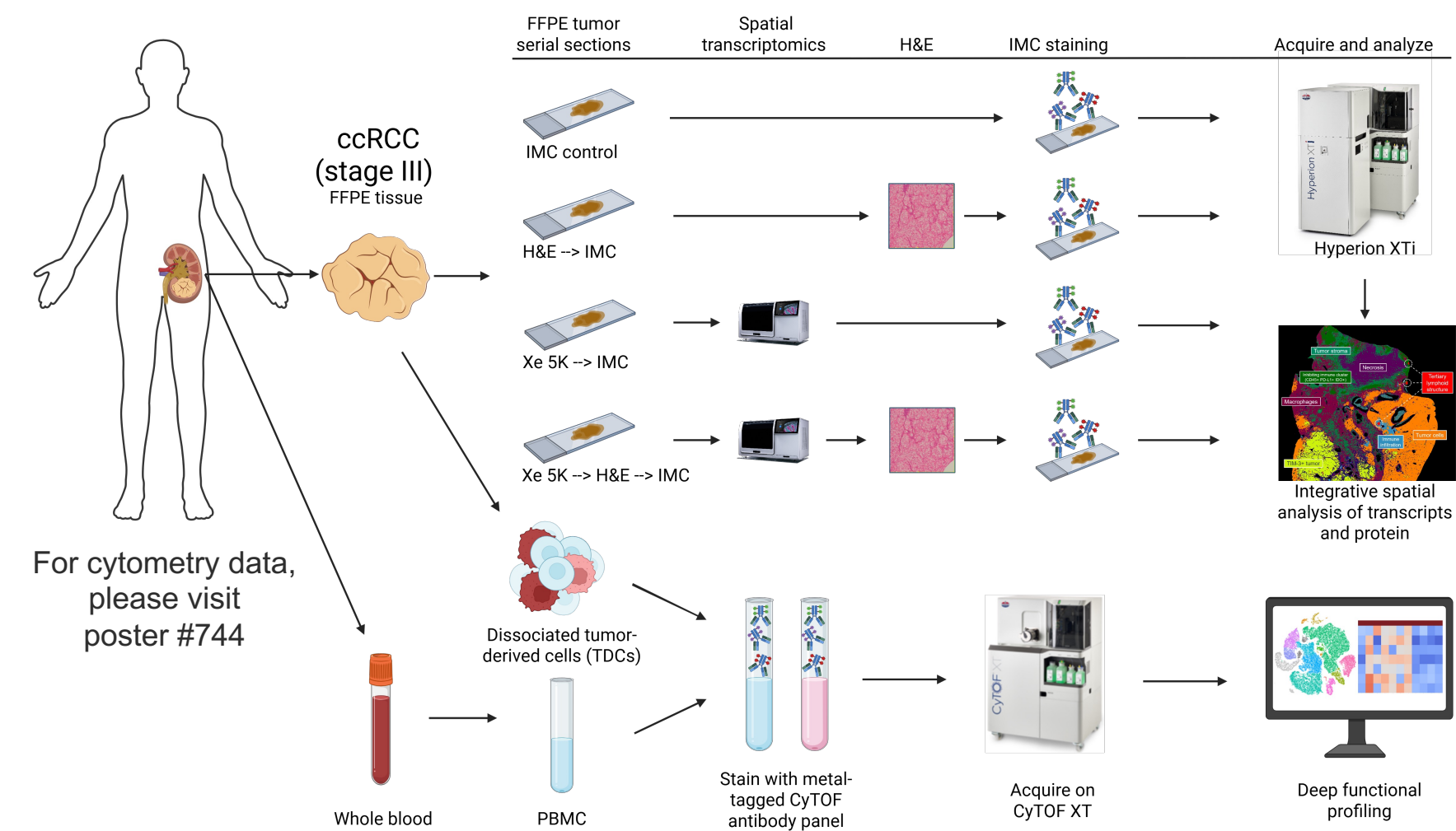


Figure 1. Integration of spatial transcriptomics and proteomics amplifies the biological insights obtained from the same sample. Proteins reveal functional information beyond what RNA alone can provide. Since tissue sections run on a spatial transcriptomic system remain largely intact after processing, the same slide can be used to obtain spatial proteomic insights on the Hyperion™ XTI Imaging System. Spatial transcriptomic data combined with Hyperion XTI data enables researchers to get a more complete picture of the biological processes in a tissue sample.

Conclusions

By integrating spatial transcriptomics with spatial proteomics using Imaging Mass Cytometry (IMC) technology, we demonstrate a **powerful multimodal and pathologist-friendly framework** for dissecting tissue architecture and cellular phenotypes *in situ*. IMC technology enables high-dimensional multiplexed protein profiling with subcellular resolution and a wide dynamic range of signal detection in combination with spatial transcriptomic approaches and H&E protocol needed for clinical pathology. The complementary insights gained from RNA and protein spatial landscapes revealed:

- Novel cellular interactions and molecular patterns that would remain undetected by spatial transcriptomics alone
- Post-transcriptional modification, activated phosphorylation states and nuclear localization of transcription factors
- Spatially organized cellular interactions linked to functional activation

Our approach underscores the value of IMC technology as a cornerstone in spatial biology, offering a robust, scalable and highly informative method for advancing systems-level understanding of tissue organization and disease pathology. Overall, the features of IMC technology make it a **clinically relevant spatial proteomic platform**, potentially opening doors for diagnostic, prognostic and therapeutic biomarker discovery in patient tissues.

Results

IMC technology successfully discovers spatial biology of FFPE tissue samples previously processed with spatial transcriptomics and H&E

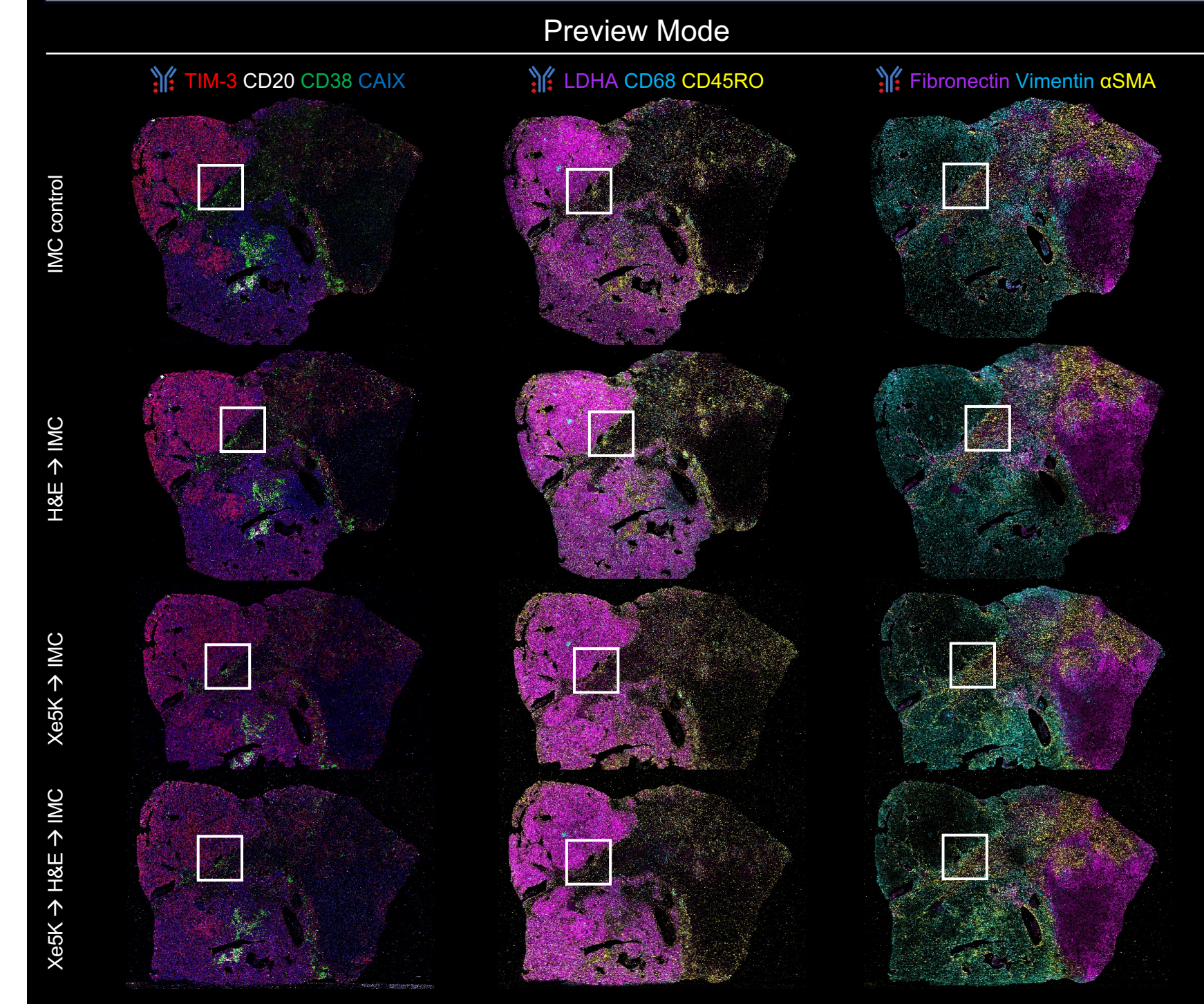


Figure 2. Preview Mode offers detection of tissue structures in FFPE tissue previously processed with spatial transcriptomics and H&E. Rendered Preview Mode images for IMC control, H&E -> IMC, Xe5K -> IMC and Xe5K -> H&E -> IMC slides demonstrate equivalent tissue architecture detection in serial sections of ccRCC tissue. Presence of tertiary lymphoid structures (CD20), activated T cells (CD38), memory T cells (CD45RO), macrophages (CD68), metabolically active tumor cells (LDHA), stromal cells (alphaSMA, vimentin) and extracellular matrix (fibronectin) can be detected in all samples. This information guides placement of regions of interest for single-cell resolution imaging with Cell Mode. Due to a step in the spatial transcriptomic protocol in which protease treatment is required, some protein antigens can be negatively impacted. Due to this, histogram adjustments were individually optimized for each image to best represent spatial biology of the tissue.

Coregistration of multimodal data provides a comprehensive view into ccRCC spatial biology

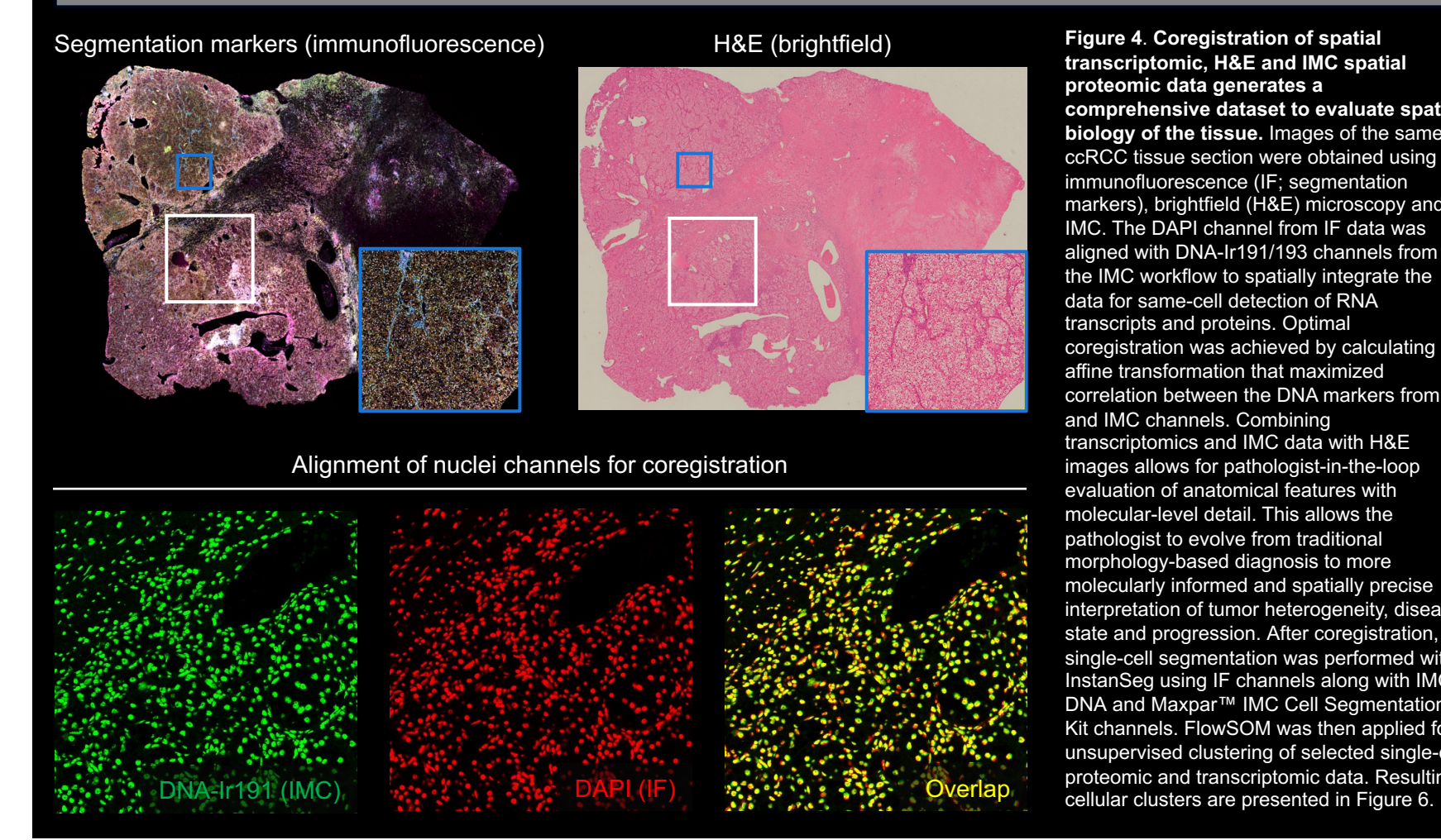


Figure 4. Coregistration of spatial transcriptomic, H&E and IMC data provides a comprehensive view into ccRCC spatial biology. Images of the same ccRCC tissue section were obtained using immunofluorescence (IF) segmentation markers, brightfield (H&E) microscopy and IMC. The DAPI channel from IF data was aligned with DNA-H191/193 channels from the IMC workflow to spatially integrate the data for same-cell detection of RNA transcripts and proteins. Optimal coregistration was achieved by calculating the affine transformation that maximized correlation between the DNA markers from IF and IMC channels. Combining transcriptomics and IMC data with H&E images allows for pathologist-in-the-loop evaluation of anatomical features with molecular-level detail. This allows the pathologist to evolve from traditional morphology-based diagnosis to more molecularly informed and spatially precise interpretation of tumor heterogeneity, disease state and progression. After coregistration, single-cell segmentation was performed with InstanSeg using IF channels along with IMC DNA and Maxpar™ IMC Cell Segmentation Kit channels. FlowSOM was then applied for unsupervised clustering of selected single-cell proteomic and transcriptomic data. Resulting cellular clusters are presented in Figure 6.

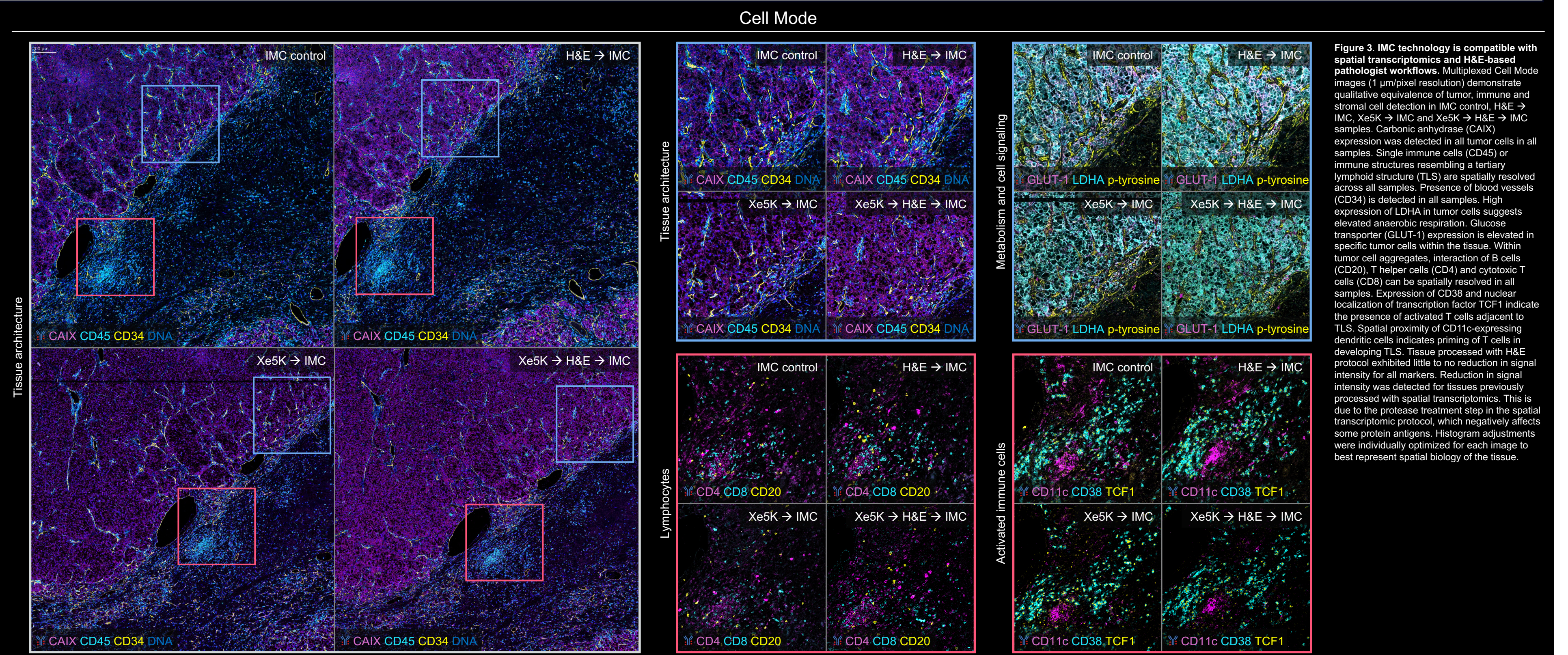


Figure 3. IMC technology is compatible with spatial transcriptomics and H&E-based pathologist workflows. Multiplexed Cell Mode images (1 μm/pixel resolution) demonstrate qualitative equivalence of tumor, immune and stromal cell detection in IMC control, H&E -> IMC, Xe5K -> IMC and Xe5K -> H&E -> IMC samples. Carbonic anhydrase (CAIX) expression was detected in all tumor cells in all samples. Single immune cells (CD45) or immune structures resembling a tertiary lymphoid structure (TLS) are spatially resolved across all samples. Presence of blood vessels (CD34) is detected in all samples. High expression of LDHA in tumor cells suggests elevated anaerobic respiration. Glucose transporter (GLUT-1) expression is elevated in specific tumor cells within the tissue. Within tumor cell aggregates, interaction of B cells (CD20), T helper cells (CD4) and cytotoxic T cells (CD8) can be spatially resolved in all samples. Expression of CD38 and nuclear localization of transcription factor TCF1 indicate the presence of activated T cells adjacent to TLS. Spatial proximity of CD11c-expressing dendritic cells indicates priming of T cells in developing TLS. Tissue processed with H&E protocol exhibited little to no reduction in signal intensity for all markers. Reduction in signal intensity was detected for tissues previously processed with spatial transcriptomics. This is due to the protease treatment step in the spatial transcriptomic protocol, which negatively affects some protein antigens. Histogram adjustments were individually optimized for each image to best represent spatial biology of the tissue.

Integrating spatial transcriptomic and proteomic data characterizes functional subtypes of tumor and immune cells in ccRCC

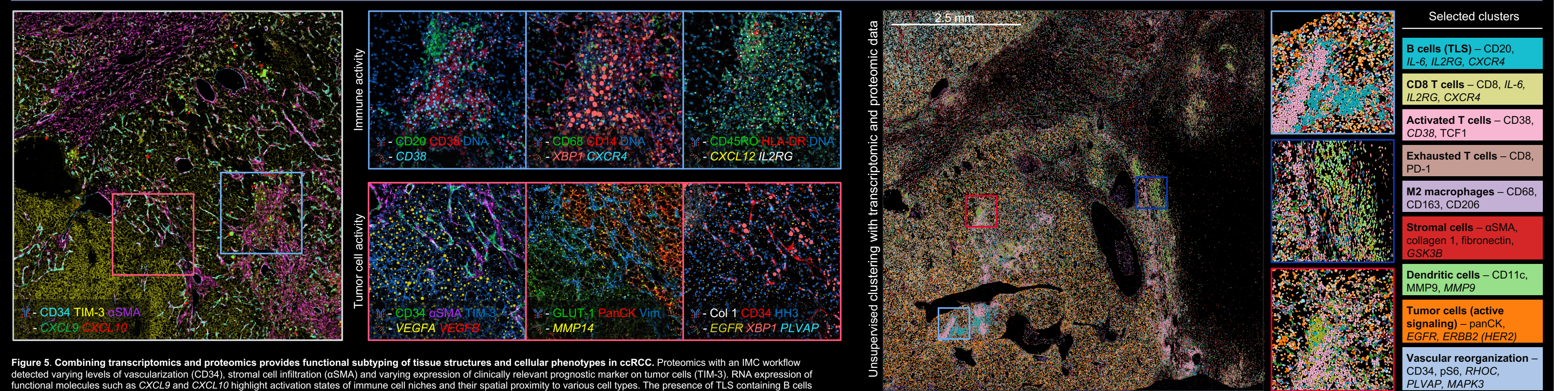


Figure 5. Unsupervised clustering with RNA and proteins provides detection of cell-cell interaction networks. Expression of cytokines (IL-6, IL2RG) in TLS indicates a robust local immune activation. Tumor cells with expression of signaling receptors suggest a differentiated cell state with high metastatic potential. The presence of signaling markers in vasculature demonstrates presence of active angiogenesis at specific locations in the tumor.

Figure 6. Combining transcriptomics and proteomics provides functional subtyping of tissue structures and cellular phenotypes in ccRCC. Proteomics with an IMC workflow detected varying levels of vascularization (CD34), stromal cell infiltration (alphaSMA) and varying expression of clinically relevant prognostic marker on tumor cells (TIM-3). RNA expression of functional molecules such as CXCL9 and CXCL10 highlight activation states of immune cell niches and their spatial proximity to various cell types. The presence of TLS containing B cells (CD20), activated T cells (CD38), macrophages (CD68, CD14), memory T cells (CD45RO) and antigen-presenting cells (HLA-DR) is detected. The activated state of TLS is delineated through the presence of transcripts for XBP1, CXCR4, CXCL12 and IL2RG. Elevated levels of VEGFA are detected in TIM-3hi tumor cell population, suggesting high angiogenic potential of vasculature. However, vascularization in TIM-3hi tumor area was low. Expression of PLVAP, a molecule involved in vascular permeability, was detected in blood vessels, indicating increased permeability associated with dysfunctionality. Expression of MMP14, a matrix protease, was detected in tissue area with high vascularization, additionally indicating reorganization of the tissue microenvironment. Italicized text - markers detected with RNA probes; non-italicized text - markers detected with antibodies.

